Journal of Advanced Marine Engineering and Technology, Vol. 46, No. 6, pp. 409~414, 2022
J. Advanced Marine Engineering and Technology (JAMET)
https://doi.org/10.5916/jamet.2022.46.6.409

ISSN 2234-7925 (Print)
ISSN 2765-4796 (Online)
Original Paper

Analysis of battery lifetime based on the inverter driving pulse

Hee-Su Kim[1] · Sung-geun Lee[†]

(Received December 5, 2022 ; Revised December 19, 2022 ; Accepted December 19, 2022)

Abstract: With the rapid increase in environmental pollution over time, the climate change has progressed rapidly, and emissions of CO_2, CH_4, N_2O, HFCs, PFCs, and SF_6 are regulated. Several factors that contribute to climate change have happened in the fields of production and means of transportation, such as ships, planes, and cars. Owing to the strengthening of international regulations, there is a great deal of interest and investment in eco-friendly transportation around the world. An electric vehicle(EV), a representative model of eco-friendly transportation, has a battery, inverter, and electric motor system. Because the main source of energy for these eco-friendly means of transportation is a battery, it is important to create an environment that can increase battery efficiency and optimize battery lifetime so that the battery can be used for a long time. The internal resistance (IR) value of the battery, which can predict the lifetime characteristics, increases owing to harmonics, ambient temperature, and chemical reactions during charge/discharge. This study analyzed the battery lifetime based on the inverter driving pulse, which affects the motor current harmonic characteristics. It was verified that, as the dead time increased, the harmonic increased, and as the harmonic increased, the IR of the battery increased, affecting the lifetime of the battery.

Keywords: Harmonics, Lithium-ion batteries, Impedance estimation, Battery internal resistance (IR)

1. Introduction

From the era of industrialization to the 20th century, the indiscriminate use of fossil fuels such as coal, oil, and natural gas, which are the main contributors to environmental pollution, has resulted in global warming. As the degree of climate change intensifies, there is a growing demand for international regulations on fossil fuels, and each country is implementing policies to encourage the use of eco-friendly energy sources. The EV is a representative field that is rapidly being replaced by eco-friendly energy. Because of the use of electricity, which is an eco-friendly alternative, EV have low noise, excellent control performance, and simple vehicle structure design. In addition, as eco-friendly policies become widely accepted, the market scale and sales volume of eco-friendly vehicles are expected to continue to increase in the near future **[1]**.

The number of EVs manufactured and used worldwide has increased annually, and accordingly, the volume of used batteries, has also increased exponentially. Though there is a need for high-capacity and high-energy batteries, more than one million batteries have been discarded since 2020. The shorter the remaining lifetime of the battery, the shorter the replacement time of the battery, and several problems such as wastage of manpower for periodic management may be caused.

To reduce the volume of waste batteries, it is necessary to use and manage batteries more efficiently. As the supply of EV expanded, the number of registered EV in Korea exceeded 100,000 in March 2020, making it difficult to dispose of waste batteries. By 2029, the number of waste batteries in domestic EV is expected to reach approximately 80,000.

Several studies have been conducted on the recycling of waste batteries. However, it is necessary to design a control circuit or prepare software that can help to use the battery for a long time. In general, it is known that the lifetime of a battery is affected not only by the current harmonics flowing in the connected circuit but also by the ambient temperature or chemical reaction. Therefore, this study analyzed the battery lifetime based on the inverter driving pulse, which affects the motor current harmonic characteristics.

† Corresponding Author (ORCID: http://orcid.org/0000-0003-2493-3916): Professor, Major of Electrical and Electronics Engineering, Korea Maritime & Ocean University, 727, Taejong-ro, Yeongdo-gu, Busan 49112, Korea, E-mail: sglee48@kmou.ac.kr, Tel: 051-410-4821
1 Researcher, Electrical and Electronics Engineering, Korea Maritime & Ocean University, E-mail: hskim@komeri.re.kr, Tel:051-400-5426

2. Theory

2.1 Total harmonic distortion (THD)

THD is expressed as the sum of all harmonic components and the ratio of the fundamental frequency. THD represents the degree of distortion owing to harmonics mixed in the waveform; the more the harmonic components, the more distorted the shape of the sine wave.

THD (%) may be expressed as the following **Equation (1)**.

$$THD = \frac{\sqrt{V_2^2+V_3^2+V_4^2+\cdots V_n^2}}{V_1} \quad (1)$$

$V_1, V_2 \sim V_n$: Amplitudes of each harmonic from the fundamental wave

Harmonics appear in nonlinear loads, which are power conversion devices, such as inverters, and rectifiers, and occur during the energy conversion process.

This study controlled the magnitude of the harmonic wave by changing the dead time, as it has a nonlinear effect on the power current when operating an inverter that controls the induction motor.

2.2 Battery deterioration

Charging and discharging must be repeated to use the battery. As the battery is charged and discharged, it is degraded by internal chemical reactions, and its lifetime is reduced. The state of health (SOH) and state of charge (SOC) were identified to determine the degree of battery degradation.

SOH refers to the health state of the battery and is a value indicating the degree of degradation as the battery is frequently used.

It is feasible to determine the degree of degradation as the battery is used, and it is difficult to accurately measure the SOH; however, there is a method of estimation using several parameters. The deterioration state of the SOH can be estimated as shown in **Equation (2)** using the consumed amount of power **[2][3][4]**.

$$\mathrm{SOH(t)} = \mathrm{SOH(0)} - \frac{1}{2NQ_{new}}\int_t^{t+\Delta t}\frac{|P_b(\tau)|}{3600}d\tau \quad (2)$$

N : Number of charge/discharge cycles

Q_{new} : Initial battery capacity

P_b : Amount of power

SOC is a value that indicates the capacity of the remaining battery to be among the total capacities. SOC 100% means fully charged, and SOC 0% means that no battery remains. Accurate figures were obtained using a battery management system (BMS) to estimate the remaining SOC.

2.3 Impedance estimation using OCV

Figure 1 shows Randles' primary battery model, and **Figure 2** shows the response of the battery terminal voltage to the charge/discharge current **[5]**.

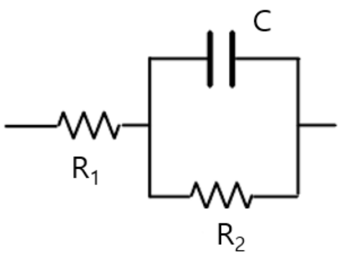

Figure 1: Equivalent circuit of Randles' model

R_1 : Battery IR

R_2 : Ionization loss resistance.

C : Double layer capacitance

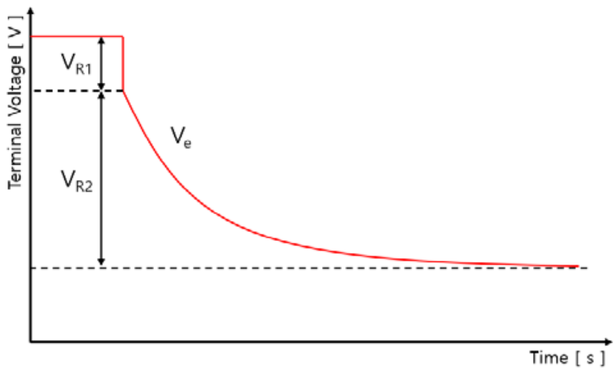

Figure 2: Estimation of battery resistance R_1 and R_2

$V_{R1} = R_1$ I

$V_{R2} = R_2$ I

$V_e = R_2 exp(-\frac{1}{R_2 C}t)$

As illustrated in **Figure 2**, when the battery is connected to the load, the load current is divided by the voltage drop V_{R1} owing to an instantaneous short circuit to calculate the IR R_1 of the battery, thereby confirming the battery lifetime **[6][7]**.

The IR of a battery can be measured using a voltage difference in a state in which a DC load is instantaneously connected to a charged battery and a voltage in an open state, or using an electrochemical impedance spectroscopy (EIS) method. In general, the lifetime of a battery is predicted using this IR value, and it is known that, as the state of the battery degrades, the IR increases **[8]**.

3. Experiment and consideration

Table 1: U_{eff} according to IGBT switching

Effective voltage vector U_{eff}	SW_a	SW_b	SW_c	V_a	V_b	V_c
U	0	0	0	0	0	0
U_0	1	0	0	2/3	-1/3	-1/3
U_{60}	1	1	0	1/3	1/3	-2/3
U_{120}	0	1	0	-1/3	2/3	-1/3
U_{180}	0	1	1	-2/3	1/3	1/3
U_{240}	0	0	1	-1/3	-1/3	2/3
U_{300}	1	0	1	1/3	-2/3	1/3
U_{360}	1	1	1	0	0	0

3.1 System configuration

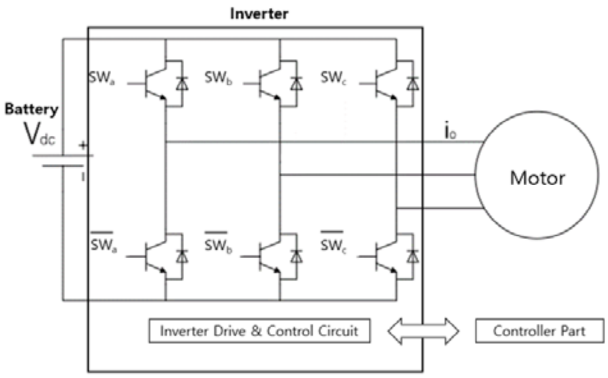

Figure 3: Diagram of EV system

A configuration diagram of the EV is shown in **Figure 3**. First, the IR value of the battery is estimated using the OCV technique. This value can be used to determine the change in the IR of the battery and to predict the degree of degradation and lifetime.

The THD is measured from the discharge current of the EV motor and compared with the estimated IR value of the battery. It checks the way the harmonic affects the battery lifetime.

The inverter includes a microprocessor (MCU), a gate driver, and an inverter circuit. The inverter control method is controlled by the spatial voltage vector, and the three-phase motor operates using a control algorithm. Space vector pulse width modulation (SVPWM) is a modulation technology that converts DC into AC and uses eight switching states in a three-phase two-level inverter to generate voltage space vectors on the space vector.

The case where the upper and lower semiconductors are operated according to the effective voltage vector U_{eff} is expressed as 1 and 0, respectively, depending on the eight switching states, as shown in **Table 1**. Depending on the phase, the three-phase a, b, and c operations show a sine wave graph with a difference of 120°and output voltage.

The block diagram of space vector is illustrated in **Figure 4** and if T_s is applied within one period through the command voltage U_{out} between the effective voltage vectors U_0 and U_{60}, U_{out} can be output, as shown in Equation (3) **[9]**.

$$U_{out}\, T_s = U_0 T_1 + U_{60} T_2 \tag{3}$$

U_{out} : Command voltage

T_s: Time at which effective voltage vector U_{eff} is applied.

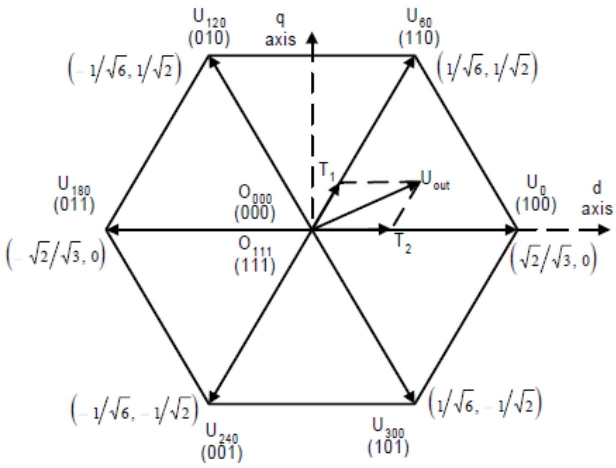

Figure 4 : Block diagram of space vector

3.2 Experiment

Figure 5 shows an experimental device for vector control of an electric motor. The experimental device consisted of a battery, a microprocessor, a gate drive, and an inverter circuit. An inverter is a device that converts the DC output voltage supplied from a battery into AC output voltage and is amplified by a gate drive to input PWM pulses to the semiconductor devices up and down of the inverter to drive an electric motor. PWM pulses are applied to SW_a and $\overline{SW_a}$ in **Figure 3**, where a section in which two pulses are not simultaneously applied is called dead time.

Table 2: Specifications of test equipment

Items	Manufacturer	Serial Number
Battery	Power Co., Ltd	PWS4S1P-2.6A
Inverter control module	TI	TMS320F28335
3-Phase motor	AMAGAWA	TS4632N2050E510D

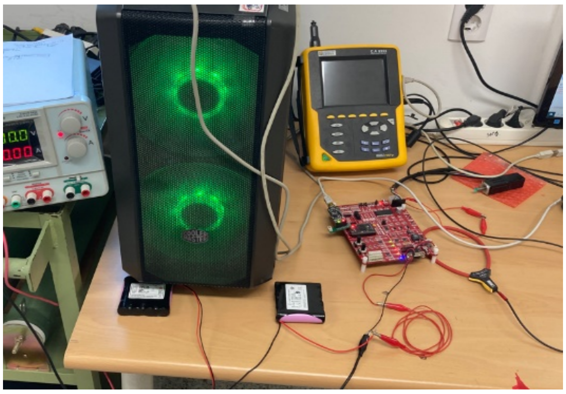

Figure 5 : Experimental setup

The module is driven by inputting a source to the JTAG emulator (XDS 100S) of SyncWorks. The battery (PWS4S1P-2.6A) configuration involves four batteries connected in series, and the battery voltage is measured using an oscilloscope. The specifications of the lithium-ion battery are presented in **Table 3**.

Table 3: Lithium-ion battery specifications

Items	Serial Number
Rated voltage	14.8 V
Nominal capacity	2,600 mAh
Charge voltage	16 V
Discharge cut-off voltage	13.6 V
Standard charge current	1,300 mA
Max. charge current	2,600 mA

For the battery discharge operation test, a 14.8 V, 2,600 mAh module composed of four batteries was used, with a discharge time per time of 330 min, and an electron load was applied after discharge to measure the IR of the battery through the instantaneous discharge of 1 A constant current. For the discharge operation test, the electric motor connected to the inverter was subjected to a no-load operation of 0.2 A at 792 rpm, and the battery discharge capacity was 0.077 C-rate. The C-rate is represented as the charge/discharge current (A) for the rated capacity (Ah); a higher C-rate indicates that a higher current is consumed.

As a result of measuring IR, as shown in **Figure 6**, it can be observed that IR itself gradually increases. It can be observed that 0.0064 Ω increased as a result of charging and discharging six times compared to the first 0.1768 Ω. It was confirmed that the IR of the battery gradually increased because of internal degradation caused by charging and discharging the battery.

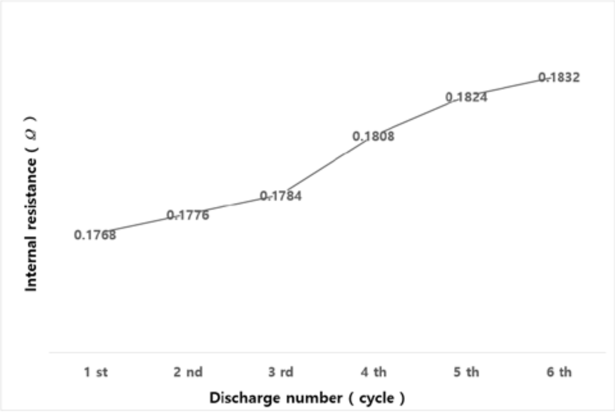

Figure 6 : IR of battery after charging and discharging

As described in Section 2.1, after charging the battery, the IR of the battery is measured under no load, and the current harmonic characteristics are verified by operating an electric motor while changing the dead time to 0.5 μs and 3.5 μs, respectively.

To relatively compare the harmonic and internal resistance values according to the dead time, a value of 0.5 μs with the small dead time and a value of 3.5 μs with the large dead time were selected.

When the dead time is operated at 0.5 μs and 3.5 μs, the average values of the harmonics flowing through the motor are 13.5 ~ 18.9 %f and 19.5 ~ 28.9 %f, respectively, and it is found that the larger the dead time, the more the current harmonics are affected.

Figure 7 shows the IR fluctuation values measured while the dead time was operated at 0.5 μs and 3.5 μs, respectively. For the operation, the fluctuation value of the IR was measured after operating for 330 minutes every time over 7 times. The reason for comparing the data values with the fluctuation in IR is that the C-rate is too low to see the change in the IR itself, hence to obtain comparable data in a short time, the change in IR is measured immediately after charging and discharging the battery.

In the case of 0.5 μs, it gradually increased from 0.008 Ω to 0.0112 Ω, and the average value was 0.0075 Ω. In addition, when it was 3.5 μs, it gradually decreased from 0.0152 Ω to 0.0136 Ω, and the average value was 0.0118 Ω.

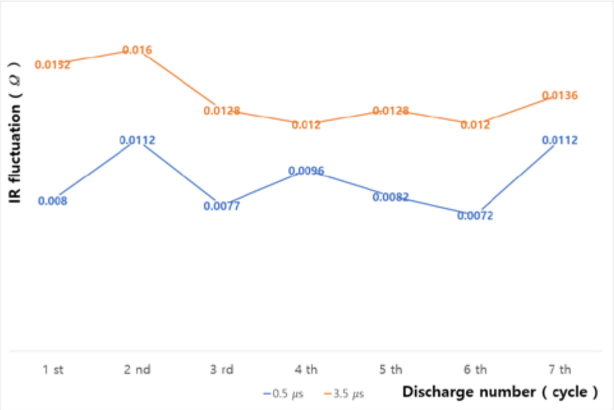

Figure 7: IR fluctuation of battery according to dead time

Comparing the graph values when the dead time is 0.5 μs and 3.5 μs, it can be found that the larger the dead time, the greater the variation in the IR.

The fluctuation value of IR is very small. Comparing the cases of 0.5 μs and 3.5 μs, it can be observed that the overall trend of increase and decrease is similar, although there is a slight difference in values.

As the increase in the IR of the battery is a parameter that promotes the aging of the battery, it is predicted that the harmonic wave increases as the dead time increases and the battery ages more.

4. Conclusion

In this study, an EV system is connected to a battery, inverter, motor, and microprocessor, and the harmonic wave and battery lifetime characteristics depending on the change in inverter dead time are analyzed. The following conclusions are drawn:

1. When the dead-time is operated at 0.5 μs and 3.5 μs, the average values of the current harmonics flowing the motor are 13.5 ~ 18.9 %f and 19.5 ~ 28.9 %f, respectively, and it is found that the larger the dead-time, the more the current harmonics are affected.
2. On repeating the battery charging and discharging six times, the IR of the battery gradually increased from 0.1768 to 0.1832 Ω owing to the internal degradation of the battery.
3. As a result of operating the dead time at 0.5 μs and 3.5 μs, respectively, within the same pulse period, the change in the average IR of the battery was measured to be 0.0075 Ω and 0.0118 Ω, respectively, and as the harmonic increased, the change in the IR increased.

In the future, it will be necessary to analyze the effect on battery lifetime from different perspectives, such as the current consumption and C-rate.

Acknowledgement

This research was an improvement of Kim Hee-Su's master's thesis (“A study on the change of battery internal resistance with inverter switching pattern and ambient temperature” Graduate school of Korea Maritime and Ocean University, Korea, 2022”).

Author Contributions

Conceptualization, H. S. Kim and S. G. Lee; Methodology, H. S. Kim; Software, H. S. Kim; ; Formal Analysis, H. S. Kim; Investigation, S. G, Lee; Data Curation, H. S. Kim; Writing—Original Draft Preparation, H. S. Kim; Writing—Review & Editing, S. G. Lee; Visualization, H. S. Kim; Supervision, S. G. Lee; Project Administration, S. G. Lee; Funding Acquisition, S. G. Lee.

References

[1] H. -K. Ku, H. -R. Seo, and J. -M. Kim, “Lithium-ion battery energy storage system for power quality improvement in electrical propulsion ships,” The Transactions of the Korean Institute of Power Electronics, vol. 20, no. 4, pp. 351-355, 2015 (in Korean).

[2] P. O. Hadi and G. Fujita, “Battery charge control by state of health estimation,” Indonesian Journal of Electrical Engineering and Computer Science, vol. 5, no. 3, pp. 508-514, 2017.

[3] J. H Park, W. C. Cha, U. R. Cho, and J. C. Kim, “State of charge estimation of Li-Ion battery based on CIM and OCV using Extended Kalman Filter,” Journal of the Korean Institute of Illuminating and Electrical Installation Engineers, vol. 28, no. 11, pp. 77-83, 2014 (in Korean).

[4] Y. M. Jung, An Enhanced OCV Reset Algorithm to Improve the Coulomb Counting Method of Li-Polymer Battery for xEVs, M. S. Thesis, Department of Electrical and Computer Engineering, Sungkyungwan university, 2014 (in Korean).

[5] J. E. B. Randles, “Kinetics of rapid electrode reactions,” Discussions of the Faraday Society, vol. 1, pp. 11-19, 1947.

[6] J. H. Kim, A Study on the Screening and Battery Packet Modelling Technique for Effective Battery Management System, Ph. D. Dissertation, Department Electrical and

Computer Engineering, Seoul National University, 2012 (in Korean).

[7] D. Y. Noh, I. S. Hwang, and J. Y. Yoo, "SOH estimation method of lithium polymer batteries using OCV," Proceedings of the KIPE Conference, pp. 269-270, 2010 (in Korean).

[8] D. Y. Noh, "A study on the SOH estimation method of lithium ion batteries using OCV," Department of Electrical and Computer Engineering, Korea University, 2011 (in Korean).

[9] B. WU, High-power converters and AC drives, Wiley interscience, pp. 95-160, 2006.